

One-loop electroweak radiative corrections to polarized Møller scattering

S.G. Bondarenko¹, L.V. Kalinovskaya², L.A. Rummyantsev², and
V.L. Yermolchyk^{2,3}

¹Bogoliubov Laboratory of Theoretical Physics, Joint Institute for Nuclear Research, Dubna,
141980 Russia

²Dzhelepov Laboratory of Nuclear Problems, Joint Institute for Nuclear Research, Dubna, 141980
Russia

³Institute for Nuclear Problems, Belarusian State University, Minsk, 220006 Belarus

March 22, 2022

Abstract

This work is devoted to a theoretical description of polarized Møller scattering. Complete one-loop electroweak radiative corrections are calculated in the helicity amplitude approach with allowance for the exact dependence on the muon mass. Numerical results are presented for integrated unpolarized and polarized cross sections as well as angular differential distributions. Calculations are performed using **ReneSANCe** Monte Carlo generator and **MCSANC** Monte Carlo integrator.

1 Introduction

The next generation of electron colliders – the International Linear Collider (ILC) [1–6], the e^+e^- Future Circular Collider (FCCee) [7–11], the Compact Linear Collider (CLIC) [12–14], and the Circular Electron Positron Collider (CEPC) [15] – will allow an extensive program of experiments with unique opportunities for precision measurements. A major advantage to fulfill this goal is the universality of linear colliders, as they can operate in four e^+e^- , e^-e^- , $e^- \gamma$ and $\gamma\gamma$ modes with strongly polarized electron and photon beams. An important feature of linear colliders is a high degree of polarization which can be obtained for electron beams.

The Møller scattering along with the Bhabha and Compton-like processes is a good candidate for luminosity measurements and the background estimation in many searches for new physics beyond the Standard Model. At high energies for the polarized Møller scattering the most advanced Monte Carlo tool is needed not only to estimate luminosity, i.e. polarized experiments CLIC [13], ILC [16], but also to study muon-muon polarized scattering at μ TRISTAN [17].

Equal lepton scattering, $e^-e^- \rightarrow e^-e^-$ was first calculated by C. Møller in 1932 [18]. There are a great number of theoretical works for description polarized case of this process [19–26]. In this series of papers the calculations are given for the QED and electroweak (EW) one-loop corrections with taking into account the polarization.

A calculation of the radiative corrections (RCs) was performed for the unpolarized Møller scattering for the experiment [27] at one-loop level [28, 29], partly at two-loop level [30] and in the first time beyond the ultra-relativistic approximation in [31].

However, all of the above-mentioned studies are not accompanied by the development of the Monte Carlo event generator which is the standard of the modern theoretical support of the high-precision experiments.

The following Monte Carlo generators currently exist, which take into account polarization at tree level: **AMEGIC++** [32], based on the helicity amplitudes and being a part of **SHERPA**; **COMPHEP** [33], using the traditional trace techniques to evaluate the matrix elements; **GRACE** [34, 35] (with the packages **BASES** and **SPRING**), calculating matrix elements via helicity amplitude techniques; **WHIZARD** [36] a software system, intended for the effective calculation of scattering cross-sections of many-particle and simulated events, where polarization is processed for both the initial and final states.

Theoretical support of experiments by the **MERADGEN** MC generator for polarized Møller scattering within QED theory is presented in [37].

In our previous works we estimated the theoretical uncertainty for the complete one-loop and leading higher-order EW corrections for e^+e^- and $\gamma\gamma$ polarized beams. The implementations of polarized Bhabha scattering [38], polarized $e^+e^- \rightarrow ZH$ [39], s -channel [40], $e^+e^- \rightarrow \gamma Z$ [41] and $\gamma\gamma \rightarrow ZZ$ [42] are available in the **ReneSANCe** MC generator [43] and the **MCSANC** integrator in the fully massive case and in total phase space.

This article is the next step in the series of **SANC** papers devoted to the implementation of one of the channels $4f \rightarrow 0$, namely, the equal lepton scattering at the one-loop level with allowance for polarization.

The $\alpha(0)$ EW scheme is used in the calculations. All the results are obtained for the center-of-mass system (c.m.s.) energies from $\sqrt{s} = 250$ GeV up to 3 TeV. The sensitivity to the initial polarization for the Born and hard photon bremsstrahlung cross sections was estimated for four beam polarization data sets:

$$\begin{aligned} (P_{e^-}, P_{e^-}) = & \\ (0, 0), (-1, -1), (-1, +1), (+1, -1), (+1, +1). & \end{aligned} \tag{1}$$

The one-loop contributions were calculated for the following degrees of polarization:

$$(P_{e^-}, P_{e^-}) = (0, 0), (\pm 0.8, \pm 0.8). \tag{2}$$

The statistical uncertainties were estimated using the **SANC** tools: **ReneSANCe** MC generator and **MCSANC** integrator.

This article consists of four Sections.

We describe the methodology of calculations of the polarized cross sections at the complete one-loop EW level within the helicity approach in Section 2 Numerical results and comparison are presented in the next Section 3. Summary is drawn in Section 4.

2 EW one-loop radiative corrections

We consider the differential cross section for processes

$$l^\pm(p_1, \chi_1) + l^\pm(p_2, \chi_2) \rightarrow l^\pm(p_3, \chi_3) + l^\pm(p_4, \chi_4) (+\gamma(p_5, \chi_5)), \quad (3)$$

with $l = e, \mu$ and arbitrary longitudinal polarization of initial particles (χ corresponds to the helicity of the particles).

Within the **SANC** system we calculate all processes using the on-mass-shell renormalization scheme in two gauges: the R_ξ gauge and the unitary gauge as a cross-check.

We apply the helicity approach (HA) to all components of the one-loop cross sections:

$$\sigma^{\text{one-loop}} = \sigma^{\text{Born}} + \sigma^{\text{virt}}(\lambda) + \sigma^{\text{soft}}(\lambda, \omega) + \sigma^{\text{hard}}(\omega), \quad (4)$$

where σ^{Born} is the Born cross section, σ^{virt} is the contribution of virtual (loop) corrections, $\sigma^{\text{soft(hard)}}$ is the soft (hard) photon emission contribution (the hard photon energy $E_\gamma > \omega$). The auxiliary parameters λ ("photon mass") and ω are canceled after summation. The corresponding expressions for the Møller scattering cross section cannot be integrated over all angles because the integral diverges at $\vartheta = 0, \pi$.

2.1 Born and virtual parts

To calculate the virtual part at the one-loop level using the procedure basement of **SANC**, we start with considering the covariant amplitude (CA). The covariant one-loop amplitude corresponds to the result of the straightforward standard calculation of all diagrams contributing to a given process at the one-loop level. The CA is represented in a certain basis made of strings of Dirac matrices and/or external momenta (structures) contracted with polarization vectors of vector bosons, $\epsilon(k)$, if any.

CA can be written in an explicit form using scalar form factors (FFs). All masses, kinematical factors and coupling constant and other parameter dependences are included into these FFs \mathcal{F}_i , but tensor structures with Lorenz indices made of strings of Dirac matrices are given by the basis.

The number of FFs is equal to the number of independent structures.

Loop integrals are expressed in terms of standard scalar Passarino-Veltman functions A_0, B_0, C_0, D_0 [44]. We presented the CA for the $4f \rightarrow 0$ process in [45], where we considered it at the one-loop level of annihilation into a vacuum. Recall that in **SANC** we always calculate any one-loop process amplitude as annihilation into vacuum with all 4 momenta incoming. Therefore, the derived universal scalar form factors for the amplitude of the process $4f \rightarrow 0$ after an appropriate permutation of their arguments can be used for the description of the next-to-leading (NLO) corrections of this particular case unfolding into t and u channels.

The virtual (Born) cross section of processes (3) can be written as follows:

$$\frac{d\sigma_{\chi_1\chi_2}^{\text{virt(Born)}}}{d\cos\vartheta_3} = \pi\alpha^2 \frac{\beta_s}{2s} |\mathcal{H}_{\chi_1\chi_2}^{\text{virt(Born)}}|^2, \quad (5)$$

where

$$|\mathcal{H}_{\chi_1\chi_2}^{\text{virt(Born)}}|^2 = \sum_{\chi_3,\chi_4} |\mathcal{H}_{\chi_1\chi_2\chi_3\chi_4}^{\text{virt(Born)}}|^2, \quad (6)$$

where m_l is the final lepton mass and $\beta_s = \sqrt{1 - \frac{4m_l^2}{s}}$, the angle ϑ_3 is the c.m.s. the angle between p_1 and p_3 .

Then we estimate the cross section as a function of eight helicity amplitudes. Helicity amplitudes depend on kinematic variables, coupling constants and seven scalar form factors. Helicity indices $\mathcal{H}_{\chi_1\chi_2\chi_3\chi_4}$ denote the signs of the fermion spin projections to corresponding momenta. Some basic definitions are $c^\pm = 1 \pm \cos \vartheta_3$, and the scattering angle ϑ_3 is related to the Mandelstam invariants t, u :

$$t = m_l^2 - \frac{s}{2}(1 - \beta_l \cos \vartheta_3), \quad (7)$$

$$u = m_l^2 - \frac{s}{2}(1 + \beta_l \cos \vartheta_3). \quad (8)$$

The presence of the electron masses gives additional terms proportional to the factor m_l , which can be considered significant in calculations at low energy.

The set of the corresponding HAs in the t channel for this case is:

$$\begin{aligned} \mathcal{H}_{\mp\mp\mp\mp} &= \frac{1}{t} \left[(c^+k - 4m_l^2)\tilde{F}_{gg} + \chi_z(t) \left((c^+k - 4m_l^2)\tilde{F}_{qq} \right. \right. \\ &\quad \left. \left. + 4(k \mp \sqrt{\lambda_e})\tilde{F}_{lu} + 2(c^+k - 4m_l^2 \mp 2\sqrt{\lambda_e})\tilde{F}_{lq} \right. \right. \\ &\quad \left. \left. + 2c^-m_l^2k \left[\tilde{F}_{qd} + (k \mp \sqrt{\lambda_e})\tilde{F}_{ld} \right] \right) \right], \end{aligned}$$

$$\begin{aligned} \mathcal{H}_{\mp--\pm} &= \sin \vartheta_3 \frac{\sqrt{sm_l}}{t} \left[\tilde{F}_{gg} + \chi_z(t) \left(\tilde{F}_{qq} + 2\tilde{F}_{lq} - k\tilde{F}_{qd} \right. \right. \\ &\quad \left. \left. - (k - \sqrt{\lambda_e})\tilde{F}_{ld} \right) \right], \end{aligned}$$

$$\mathcal{H}_{\pm++\mp} = -\mathcal{H}_{\mp--\pm}(\sqrt{\lambda_e} \rightarrow -\sqrt{\lambda_e}),$$

$$\begin{aligned} \mathcal{H}_{\mp\mp\pm\pm} &= -\frac{m_l^2}{t} \left[2c^+\tilde{F}_{gg} + \chi_z(t) \left(2c^+(\tilde{F}_{qq} + 2\tilde{F}_{lq}) \right. \right. \\ &\quad \left. \left. + 8\tilde{F}_{lu} - sc^+(\tilde{F}_{ld} + \tilde{F}_{qd}) \right) \right], \end{aligned}$$

$$\mathcal{H}_{\mp\pm\mp\pm} = -\frac{m_l^2}{t} \left[2c^+ \tilde{F}_{gg} + \chi_Z(t) \left(2c^+ (\tilde{F}_{qq} + 2\tilde{F}_{lq}) - sc^+ (\tilde{F}_{ld} + \tilde{F}_{qd}) \right) \right],$$

$$\mathcal{H}_{-\mp\pm-} = -\mathcal{H}_{+\mp\pm+},$$

$$\mathcal{H}_{+\mp\pm+} = \sin \vartheta_3 \frac{\sqrt{s} m_l}{t} \left[\tilde{F}_{gg} + \chi_Z(t) \left(\tilde{F}_{qq} + 2\tilde{F}_{lq} - 2m_l^2 (\tilde{F}_{ld} + \tilde{F}_{qd}) \right) \right],$$

$$\mathcal{H}_{\mp\pm\pm\mp} = \frac{c^-}{t} \left[k \tilde{F}_{gg} + \chi_Z(t) \left(k (\tilde{F}_{qq} + 2\tilde{F}_{lq}) - 2m_l^2 [(k \pm \sqrt{\lambda_e}) \tilde{F}_{ld} + k \tilde{F}_{qd}] \right) \right].$$

Here $\chi_Z(t)$ is the Z/γ propagator ratio:

$$\chi_Z(t) = \frac{1}{4s_W^2 c_W^2} \frac{t}{t - M_Z^2}. \quad (9)$$

Note that *tilded* FFs absorb couplings, which leads to a compactification of formulas for the amplitude, while explicit expressions will be given for *untilded* quantities.

The expressions for *tilded* FFs are

$$\begin{aligned} \tilde{F}_{gg} &= (I_l^{(3)})^2 F_{gg}(s, t, u), \\ \tilde{F}_{ll} &= \delta_l^2 F_{ll}(s, t, u), \\ \tilde{F}_{qq} &= I_l^{(3)} \delta_l F_{qq}(s, t, u), \\ \tilde{F}_{lq} &= \delta_l I_l^{(3)} F_{lq}(s, t, u), \\ \tilde{F}_{ql} &= \delta_l I_l^{(3)} F_{ql}(s, t, u), \\ \tilde{F}_{ld} &= (I_l^{(3)})^2 F_{ld}(s, t, u), \\ \tilde{F}_{qd} &= \delta_l I_l^{(3)} F_{qd}(s, t, u). \end{aligned} \quad (10)$$

We also use the coupling constants

$$I_l^{(3)}, \sigma_l = v_l + a_l, \delta_l = v_l - a_l, s_W = \frac{e}{g}, c_W = \frac{M_W}{M_Z}$$

with $l = e, \mu$.

In order to get HAs for the Born level, one should set $F_{gg,ll,lq,ql,qq} = 1$ and $F_{ld,qd} = 0$.

2.2 Real photon emission corrections

The real corrections consist of soft and hard radiative contributions. They are calculated using the bremsstrahlung modules. The soft bremsstrahlung radiation has a Born-like kinematics, while the phase space of hard radiation has an extra particle – photon.

The soft bremsstrahlung radiation has the following form:

$$\begin{aligned} \sigma^{\text{soft}} = & -Q_e^2 \frac{2\alpha}{\pi} \sigma^{\text{Born}} \left[\left(1 + \frac{1 - 2m_l^2/s}{\beta_s} \ln x^2 \right) \ln \left(\frac{4\omega^2}{\lambda^2} \right) \right. \\ & + \frac{1}{\beta_s} \left[-\ln x^2 + (1 - 2m_l^2/s) \left(\text{Li}_2(1 - x^2) \right. \right. \\ & \left. \left. - \text{Li}_2 \left(1 - \frac{1}{x^2} \right) \right) \right] - F(t) - F(u) \right], \end{aligned} \quad (11)$$

were

$$\begin{aligned} F(I) = & \frac{1 - 2m_l^2/I}{\beta_I} \left[\ln y_I \ln \left(\frac{4\omega^2}{\lambda^2} \right) + \text{Li}_2 \left(1 - \frac{y_I x}{z_I} \right) \right. \\ & \left. - \text{Li}_2 \left(1 - \frac{x}{z_I} \right) + \text{Li}_2 \left(1 - \frac{y_I}{z_I x} \right) - \text{Li}_2 \left(1 - \frac{1}{z_I x} \right) \right], \\ & \beta_I = \sqrt{1 - \frac{4m_l^2}{I}}, \quad x = \frac{\sqrt{s} 1 + \beta_s}{m_l 2}, \\ & y_I = 1 - \frac{I 1 + \beta_I}{m_l^2 2}, \quad z_I = \frac{m_l}{\sqrt{s}} (1 + y_I), \end{aligned}$$

with $I = t, u$.

In presenting the results we used our universal massive module for the hard photon bremsstrahlung for $4f \rightarrow 0$ [40] by appropriate unfolding it in the right channel.

3 Numerical results

3.1 Tree level

In this Section calculated polarized cross sections at tree level for the Born and hard photon bremsstrahlung are compared with the results of the CalcHEP [33] and WHIZARD [36, 46, 47] codes.

The results are calculated in the $\alpha(0)$ EW scheme with fixed 100% polarized initial states for $\sqrt{s} = 250$ GeV and angular cuts $|\cos \vartheta_e| \leq 0.9$. For the hard bremsstrahlung cross sections, an additional cut on the photon energy $E_\gamma \geq \omega = 10^{-4} \sqrt{s}/2$ is applied.

The Born results agree in all digits for all codes, and therefore the table is omitted. The hard bremsstrahlung results are shown in Table 1. Very good agreement within statistical errors with the above mentioned codes is found.

Table 1: Table 1. The tuned triple comparison between **SANC** (the second column), **WHIZARD** (the third column), and **CalcHEP** (the fourth column) and **SANC** results for the hard bremsstrahlung cross section

P_{e^-}, P_{e^-}	S	W	C
0, 0	170.12(1)	170.13(1)	170.11(2)
-1, -1	284.58(1)	284.58(1)	284.55(2)
-1, 1	74.00(1)	74.00(1)	74.00(2)
1, -1	74.01(1)	74.02(1)	74.00(2)
1, 1	247.90(1)	247.90(1)	247.86(2)

3.2 One-loop level

In this Section we show the study of the complete one-loop EW RCs and polarization effects for Møller scattering in high-energy regions. Numerical estimates are presented for the total (integrated) cross sections (σ , pb) and relative corrections (δ , %) as well as for the differential distribution as function of the scattering angle $\cos\vartheta_3$. The channels e^- ($e^-e^- \rightarrow e^-e^-(\gamma)$) and μ^+ ($\mu^+\mu^+ \rightarrow \mu^+\mu^+(\gamma)$) of reaction (3) are considered below.

3.2.1 Integrated cross sections

CLIC would provide high-luminosity e^-e^- collisions covering a centre-of-mass energy range from 380 GeV to 3 TeV. They are three main c.m.s. energy stages at \sqrt{s}_{CLIC} : 380 GeV, 1.5 TeV and 3 TeV.

The ILC offers many opportunities for measurements with collider energies from 90 GeV to 1 TeV. Three main c.m.s. energy stages can be distinguished – \sqrt{s}_{ILC} : 250 GeV, 500 GeV, and 1 TeV, with electron polarization of $P_{e^-} = \pm 0.8$.

Table 2 presents the integrated Born and one-loop cross section in pb and relative corrections in percent for the e^- -channel for c.m.s. energy $\sqrt{s}_{\text{ILC\&CLIC}}$ and set (2) of the initial particle polarization degrees in the $\alpha(0)$ EW scheme.

Under the μ TRISTAN experimental conditions, the energy is assumed to be $\sqrt{s}_{\mu\text{TRISTAN}}$: 0.6, 1, 2 TeV and the polarization of both beams will reach $P_{\mu^+} = \pm 0.8$ for the μ^+ -channel. Table 3 presents the same observables as in Table 2 in the conditions of the μ TRISTAN experiment.

As it seen in Tables 2 and 3, the use of the polarized beams significantly increases the cross section. At the same time the RCs increase at $P_{e^-} = (0.8, 0.8)$ and reduce at $P_{e^-} = (-0.8, -0.8)$ comparing to the unpolarized case in the region of c.m.s. energies $\sqrt{s} = 250\text{--}1000$ GeV. At higher c.m.s. energies the polarization $P_{e,\mu} = (\pm 0.8, \pm 0.8)$ increases the cross section as well, but the absolute value of the relative correction became larger than for the unpolarized one.

3.2.2 Differential cross sections

At Figures 1 and 2 the differential distributions for the LO and EW NLO cross sections (in pb) as well as the relative corrections (in %) are shown for the e^- - and μ^+ -channels for the

Table 2: Table 2. Integrated Born and one-loop cross section in pb and relative corrections in percent for e^- -channel scattering for c.m.s. energy $\sqrt{s}_{\text{ILC\&CLIC}}$ and set (2) of the initial particle polarization degrees in the $\alpha(0)$ EW scheme

P_{e^-}, P_{e^-}	0, 0	0.8, 0.8	-0.8, -0.8
$\sqrt{s} = 250$ GeV			
σ^{Born} , pb	94.661(1)	120.152(1)	136.377(1)
$\sigma^{\text{one-loop}}$, pb	103.906(2)	134.976(2)	147.224(2)
δ , %	9.77(1)	12.34(1)	7.95(1)
$\sqrt{s} = 380$ GeV			
σ^{Born} , pb	42.969(1)	55.739(1)	65.487(1)
$\sigma^{\text{one-loop}}$, pb	47.327(1)	63.264(1)	70.345(1)
δ , %	10.14(1)	13.50(1)	7.42(1)
$\sqrt{s} = 500$ GeV			
σ^{Born} , pb	25.498(1)	33.430(1)	39.984(1)
$\sigma^{\text{one-loop}}$, pb	28.068(1)	38.171(2)	42.627(2)
δ , %	10.08(1)	14.18(1)	6.61(1)
$\sqrt{s} = 1$ TeV			
σ^{Born} , pb	6.657(1)	8.850(1)	10.865(1)
$\sigma^{\text{one-loop}}$, pb	7.218(1)	10.229(1)	11.104(1)
δ , %	8.42(1)	15.58(1)	2.20(1)
$\sqrt{s} = 1.5$ TeV			
σ^{Born} , pb	2.992(1)	3.989(1)	4.928(1)
$\sigma^{\text{one-loop}}$, pb	3.185(1)	4.635(1)	4.827(1)
δ , %	6.46(1)	16.19(1)	-2.06(1)
$\sqrt{s} = 3$ TeV			
σ^{Born} , pb	0.7536(1)	1.007(1)	1.249(1)
$\sigma^{\text{one-loop}}$, pb	0.7665(1)	1.177(1)	1.103(1)
δ , %	1.71(1)	16.94(1)	-11.70(1)

c.m.s. energies $\sqrt{s} = 250, 1000$ GeV as a function of $\cos \theta_3$.

The differential distributions over $\cos \theta_3$ are symmetric for all c.m.s. energies and the maximum of the relative corrections is at the zero angle while the minimum is close to the $|\cos \theta_3| = 1$. This is due to dominance of the Born contribution in the $|\cos \theta_3| \approx 1$ region due to a photon propagator $1/t(1/u)$.

It should be noted that while the integrated relative corrections for the c.m.s. energy $\sqrt{s} = 1000$ GeV for the e^- - and μ^+ -channels differ by 0.4% (see Tables 2,3) the differential difference is larger, being about 5-6 % at $\cos \theta_3 = 0$.

Table 3: Table 3. Integrated Born and one-loop cross section in pb and relative corrections in percent for the μ^+ -channel for c.m.s. energy $\sqrt{s}_{\mu\text{TRISTAN}}$ and set (2) of the initial particle polarization degrees in the $\alpha(0)$ EW scheme

P_{μ^+}, P_{μ^+}	0, 0	0.8, 0.8	-0.8, -0.8
$\sqrt{s} = 600 \text{ GeV}$			
$\sigma^{\text{Born}}, \text{ pb}$	17.974(1)	23.690(1)	28.601(1)
$\sigma^{\text{one-loop}}, \text{ pb}$	19.715(1)	27.064(1)	30.160(1)
$\delta, \%$	9.69(1)	14.24(1)	5.45(1)
$\sqrt{s} = 1 \text{ TeV}$			
$\sigma^{\text{Born}}, \text{ pb}$	6.6572(1)	8.8497(1)	10.8648(1)
$\sigma^{\text{one-loop}}, \text{ pb}$	7.2019(1)	10.1930(1)	11.0589(2)
$\delta, \%$	8.18(1)	15.18(1)	1.79(1)
$\sqrt{s} = 2 \text{ TeV}$			
$\sigma^{\text{Born}}, \text{ pb}$	1.6903(1)	2.2559(1)	2.7935(1)
$\sigma^{\text{one-loop}}, \text{ pb}$	1.7646(1)	2.6195(1)	2.6210(1)
$\delta, \%$	4.40(1)	16.12(1)	-6.17(1)

4 Summary

We computed the NLO contributions RCs due to QED and purely weak corrections and implement them into a fully differential Monte Carlo event generator **ReneSANCe** and **MCSANC** integrator.

We presented explicit expressions for HAs to evaluate virtual and soft parts for Møller scattering. We used our previous module for HAs of the hard photon bremsstrahlung [40]. We showed the results of interest for unpolarized FCCee and polarized ILC, CLIC, $\mu\text{TRISTAN}$ experiments.

Our results show that it is necessary to include more than one-loop corrections to ensure the required level of the theoretical support.

The established **SANC** framework allows us to investigate the one-loop and higher-order corrections for any polarization, estimate the contribution of the selected helicity state, and take into account mass effects.

5 Funding

This research was supported by the Russian Foundation for Basic Research, project N 20-02-00441.

References

- [1] ILC homepages — <https://www.linearcollider.org/ILC>.

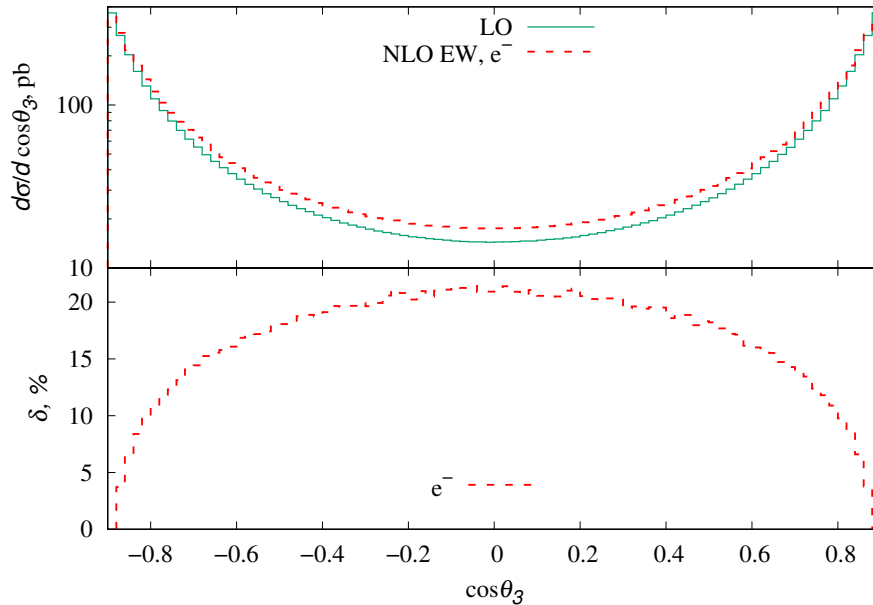


Figure 1: Fig. 1. The LO and NLO EW unpolarized cross sections (upper panel) and relative corrections (lower panel) of the e^- -channel for the c.m.s. energy $\sqrt{s} = 250$ GeV as a function of $\cos\theta_3$

- [2] A. Irlles, R. Poschl, F. Richard, and H. Yamamoto, “Complementarity between ILC250 and ILC-GigaZ”, in *Linear Collider Community Meeting Lausanne, Switzerland, April 8-9, 2019*, 2019, 1905.00220.
- [3] A. Arbey *et al.*, *Eur. Phys. J.* **C75** (2015), no. 8 371, 1504.01726.
- [4] H. Baer, T. Barklow, K. Fujii, Y. Gao, A. Hoang, S. Kanemura, J. List, H. E. Logan, A. Nomerotski, M. Perelstein, *et al.*, 1306.6352.
- [5] ECFA/DESY LC Physics Working Group Collaboration, E. Accomando *et al.*, *Phys. Rept.* **299** (1998) 1–78, hep-ph/9705442.
- [6] CLIC Physics Working Group Collaboration, E. Accomando *et al.*, “Physics at the CLIC multi-TeV linear collider”, in *Proceedings, 11th International Conference on Hadron spectroscopy (Hadron 2005): Rio de Janeiro, Brazil, August 21-26, 2005*, 2004, hep-ph/0412251.
- [7] FCC-ee homepages — <http://tlep.web.cern.ch>.
- [8] FCC Collaboration, A. Abada *et al.*, *Eur. Phys. J. ST* **228** (2019), no. 5 1109–1382.
- [9] FCC Collaboration, A. Abada *et al.*, *Eur. Phys. J.* **C79** (2019), no. 6 474.
- [10] A. Blondel and P. Janot, 1912.11871.

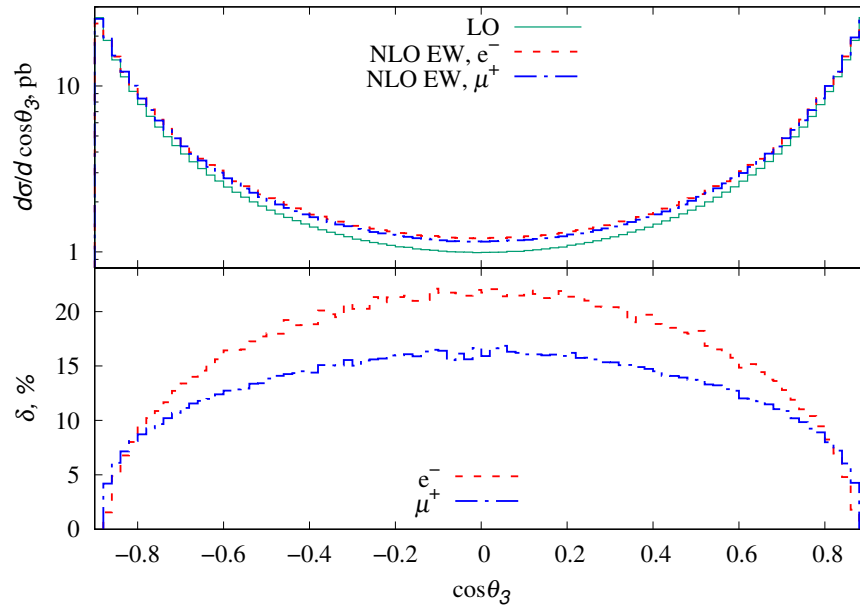


Figure 2: Fig. 2. The LO and NLO EW unpolarized cross sections (upper panel) and relative corrections (lower panel) of the e^- - and μ^+ -channels for the c.m.s. energy $\sqrt{s} = 1000$ GeV as a function of $\cos\theta_3$

- [11] A. Blondel *et al.*, “Standard model theory for the FCC-ee Tera-Z stage”, in *Mini Workshop on Precision EW and QCD Calculations for the FCC Studies : Methods and Techniques CERN, Geneva, Switzerland, January 12-13, 2018*, vol. 3, CERN, CERN, Geneva, 2019, 1809.01830.
- [12] CLIC homepages — <http://clic-study.web.cern.ch>.
- [13] CLIC, CLICdp Collaboration, M. J. Boland *et al.*, 1608.07537.
- [14] CLICdp, CLIC Collaboration, T. K. Charles *et al.*, *CERN Yellow Rep. Monogr.* **1802** (2018) 1–98, 1812.06018.
- [15] CEPC homepages — <http://cepc.ihep.ac.cn>.
- [16] K. Fujii *et al.*, 2007.03650.
- [17] Y. Hamada, R. Kitano, R. Matsudo, H. Takaura, and M. Yoshida, 2201.06664.
- [18] C. Møller, *Annalen der Physik* **14** (1932).
- [19] S. Jadach and B. F. L. Ward, *Phys. Rev. D* **54** (1996) 743–749.
- [20] N. M. Shumeiko and J. G. Suarez, *J. Phys. G* **26** (2000) 113–127, hep-ph/9912228.

- [21] J. C. Montero, V. Pleitez, and M. C. Rodriguez, *Phys. Rev. D* **58** (1998) 094026, hep-ph/9802313.
- [22] A. Denner and S. Pozzorini, *Eur. Phys. J. C* **7** (1999) 185–195, hep-ph/9807446.
- [23] A. Czarnecki and W. J. Marciano, *Int. J. Mod. Phys. A* **15** (2000) 2365–2376, hep-ph/0003049.
- [24] G. Alexander and I. Cohen, *Nucl. Instrum. Meth. A* **486** (2002) 552–567, hep-ex/0006007.
- [25] F. J. Petriello, *Phys. Rev. D* **67** (2003) 033006, hep-ph/0210259.
- [26] A. Ilyichev and V. Zykunov, *Phys. Rev. D* **72** (2005) 033018, hep-ph/0504191.
- [27] MOLLER Collaboration, J. Benesch *et al.*, 1411.4088.
- [28] A. Aleksejevs, S. Barkanova, A. Ilyichev, and V. Zykunov, *Phys. Rev. D* **82** (2010) 093013, 1008.3355.
- [29] A. I. Ahmadov, Y. M. Bystritskiy, E. A. Kuraev, A. N. Ilyichev, and V. A. Zykunov, *Eur. Phys. J. C* **72** (2012) 1977, 1201.0460.
- [30] A. G. Aleksejevs, S. G. Barkanova, Y. M. Bystritskiy, E. A. Kuraev, and V. A. Zykunov, *Phys. Part. Nucl. Lett.* **13** (2016), no. 3 310–317, 1508.07853.
- [31] I. Akushevich, H. Gao, A. Ilyichev, and M. Meziane, *Eur. Phys. J. A* **51** (2015), no. 1 1.
- [32] F. Krauss, R. Kuhn, and G. Soff, *JHEP* **02** (2002) 044, hep-ph/0109036.
- [33] A. Belyaev, N. D. Christensen, and A. Pukhov, *Comput. Phys. Commun.* **184** (2013) 1729–1769, 1207.6082.
- [34] F. Yuasa *et al.*, *Prog. Theor. Phys. Suppl.* **138** (2000) 18–23, hep-ph/0007053.
- [35] G. Belanger, F. Boudjema, J. Fujimoto, T. Ishikawa, T. Kaneko, K. Kato, and Y. Shimizu, *Phys. Rept.* **430** (2006) 117–209, hep-ph/0308080.
- [36] W. Kilian, T. Ohl, and J. Reuter, *Eur. Phys. J. C* **71** (2011) 1742, 0708.4233.
- [37] A. Afanasev, E. Chudakov, A. Ilyichev, and V. Zykunov, *Comput. Phys. Commun.* **176** (2007) 218–231, hep-ph/0603027.
- [38] D. Bardin, Y. Dydyshka, L. Kalinovskaya, L. Rumyantsev, A. Arbuzov, R. Sadykov, and S. Bondarenko, *Phys. Rev. D* **98** (2018), no. 1 013001, 1801.00125.
- [39] S. Bondarenko, Y. Dydyshka, L. Kalinovskaya, L. Rumyantsev, R. Sadykov, and V. Yermolchyk, *Phys. Rev. D* **100** (2019), no. 7 073002, 1812.10965.

- [40] S. Bondarenko, Y. Dydyshka, L. Kalinovskaya, R. Sadykov, and V. Yermolchyk, *Phys. Rev. D* **102** (2020), no. 3 033004, 2005.04748.
- [41] S. Bondarenko, Y. Dydyshka, L. Kalinovskaya, L. Rumyantsev, R. Sadykov, and V. Yermolchyk, 2111.11490.
- [42] S. Bondarenko, L. Kalinovskaya, and A. Sapronov, 2201.04350.
- [43] R. Sadykov and V. Yermolchyk, *Comput. Phys. Commun.* **256** (2020) 107445, 2001.10755.
- [44] G. Passarino and M. J. G. Veltman, *Nucl. Phys. B* **160** (1979) 151–207.
- [45] A. Andonov, D. Bardin, S. Bondarenko, P. Christova, L. Kalinovskaya, and G. Nanava, *Phys. Part. Nucl.* **34** (2003) 577–618, [Fiz. Elem. Chast. Atom. Yadra 34,1125(2003)], hep-ph/0207156.
- [46] T. Ohl, “WHiZard and O’Mega”, in *Proceedings, LoopFest V: Radiative Corrections for the International Linear Collider: Multi-loops and Multi-legs: SLAC, Menlo Park, California, June 19-21, 2006*, 2006.
- [47] W. Kilian, S. Brass, T. Ohl, J. Reuter, V. Rothe, P. Stienemeier, and M. Utsch, “New Developments in WHIZARD Version 2.6”, in *International Workshop on Future Linear Collider (LCWS2017) Strasbourg, France, October 23-27, 2017*, 2018, 1801.08034.